

# X-ray Emission from the Born-Again Planetary Nebula Abell 30

Martín A. Guerrero<sup>1</sup>

<sup>1</sup> Instituto de Astrofísica de Andalucía, IAA-CSIC, c/ Glorieta de la Astronomía s/n, 18008 Granada, Spain

## Abstract

The planetary nebula (PN) Abell 30 underwent a very late thermal pulse that resulted in the ejection of knots of hydrogen-poor material. *ROSAT* detected soft X-ray emission from these knots. We present deep *Chandra* and *XMM-Newton* observations that show this X-ray emission to consist of two components: a point-source at the central star and diffuse emission associated with the hydrogen-poor knots and the cloverleaf structure inside the nebular shell. The spatial distribution and spectral properties of the diffuse X-ray emission suggest that it is generated by the shock-heated plasma produced by the interaction of the present stellar wind with the hydrogen-poor ejecta of the born-again event. Charge-exchange reactions between the ions of the stellar winds and the born-again ejecta may also contribute to this emission. The origin of the X-ray emission from the central star of A 30 is puzzling: shocks in the present fast stellar wind and photospheric emission can be ruled out, while the development of a new, compact hot bubble confining the fast stellar wind seems implausible.

## 1 Introduction

Planetary nebulae (PNe) consist of stellar material ejected by low- and intermediate-mass stars. In the canonical interacting stellar winds (ISW) model of PN formation, the envelope of a star is stripped off through a slow and dense wind and, as the star evolves off the asymptotic giant branch (AGB), this material is subsequently swept up by a fast stellar wind to form a PN [14, 1]. As the nebula expands, the envelope is compressed and evolved PNe are expected to display a low density, low surface brightness shell with limb-brightened morphology [18].

Abell 30 (a.k.a. A 30, PN G208.5+33.2) is a PN with a hydrogen-deficient central star (CSPN) of spectral type [WC]-PG1159 (also termed as “weak emission line stars”). The nebula appears in  $H\alpha$  as a limb-brightened, presumably spherical shell  $\sim 2'$  in size. The

spherically symmetric limb-brightened morphology, the low surface brightness and the low electron density of this shell [7] are consistent with the expectations for an evolved object in the ISW model of PN formation.

Deep [O III] images of A 30 reveal that this round nebular shell is filled by a delicate system of arc-like features that extend up to  $\sim 30''$  from the central star and depict a cloverleaf pattern [12]. More remarkably, *HST* Wide Field Planetary Camera 2 (WFPC2) [O III] images detect a series of knots just a few arcsecs from the central star that are distributed along a disk and two bipolar outflows [3, 5]. Spectroscopic observations of these knots have revealed their peculiar composition, with He/H ratios as high as 20 [10, 13], inspiring the born-again PN scenario [11], where a very late thermal pulse (VLTP) of the central stars induced by the rapid fusion of He in its envelope into C and O leads to the ejection of newly processed material.

Unlike most PNe, whose present fast stellar winds blow a shell of material consist of the slow AGB wind, in a born-again PN we witness the interaction of the stellar wind with dense clumps of material close to the central star. The H-poor material ejected by the star during the born-again event will be photo-evaporated by the ionizing stellar radiation and swept up by the present fast stellar wind. A 30 provides an excellent opportunity to study processes of mass-loading of a stellar wind.

## 2 X-ray Observations

A born-again event can rejuvenate the PN's X-ray emission, as the mixture of shocked stellar wind and evaporated material is expected to emit X-rays [3]. Indeed, serendipitous *ROSAT* PSPC observations of A 30 revealed a source of soft X-ray emission from a plasma at a temperature  $\sim 3 \times 10^5$  K [4]. Follow-up HRI observations showed a central point source and hints of diffuse emission [5]. We have obtained new X-ray observations of A 30 using *XMM-Newton* (PI: Hamann) and *Chandra* (PI: Chu) with net exposure times  $\sim 31$  ks for *XMM-Newton* EPIC-MOS and RGS,  $\sim 25$  ks for *XMM-Newton* EPIC-pn, and 96.1 ks for *Chandra* ACIS-S.

The spatial distribution of the X-ray emission revealed in the X-ray images show distinct features that can be associated with different nebular and stellar components of A 30 (Fig. 1). *XMM-Newton* detects a bright, soft ( $< 0.6$  keV) source at the CSPN with an EPIC-pn count rate in the 0.22-0.6 keV energy band of  $39.6 \pm 1.3$  counts  $\text{ks}^{-1}$ . *Chandra* also detects this point source with a count rate of  $1.80 \pm 0.14$  counts  $\text{ks}^{-1}$  in the same energy band. In addition, *XMM-Newton* confirms the presence of faint extended emission at distances  $\geq 13''$  that fills the [O III] petal-like features, while *Chandra* suggests tantalizing evidence of emission associated with the southwest cometary knots.

The X-ray spectral properties suggest that line emission dominates, with very little continuum contribution. The spectrum of the diffuse emission (Fig. 2-*left*) has been modeled using an absorbed optically thin plasma emission model, adopting [15] chemical abundances and a foreground hydrogen column density ( $N_{\text{H}}$ ) of  $5 \times 10^{20}$   $\text{cm}^{-2}$  [4] with best-fit parameters  $T_{\text{X}} \approx 7.9 \times 10^5$  K and  $L_{\text{X}} \approx 6.0 \times 10^{31}$   $\text{erg s}^{-1}$  ( $d=2.4$  kpc). This model, however, does not

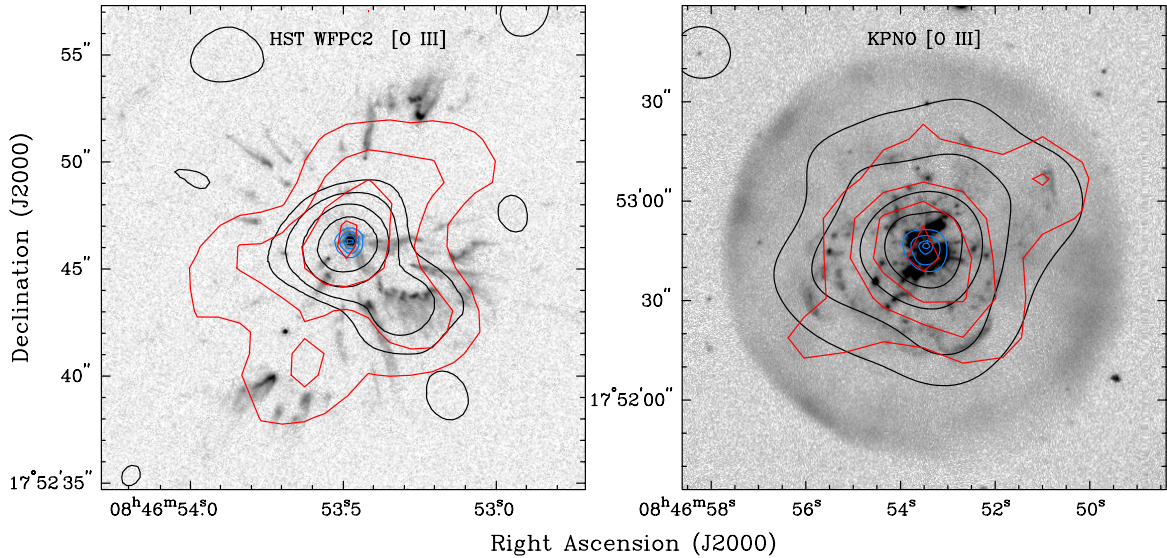


Figure 1: Optical [O III] narrow-band images of A 30 overplotted by X-ray contours: *HST* WFPC2 image overplotted by *Chandra* ACIS-S (blue and black) and *ROSAT* HRI (red) contours (*left*) and ground-based image overplotted by *XMM-Newton* EPIC (blue and black) and *ROSAT* PSPC (red) contours (*right*). Red and blue contours have been set at 95%, 75%, 50%, and 25% of the peak intensity, whereas the black contours correspond to  $5\sigma$ ,  $10\sigma$ ,  $25\sigma$ , and  $100\sigma$  above the background level for the *Chandra* ACIS-S image, and  $10\sigma$ ,  $25\sigma$ ,  $50\sigma$ , and  $100\sigma$  above the background level for the *XMM-Newton* EPIC image.

provide a good fit to the spectrum of the CSPN (Figure 1-*right*) that shows emission excess at  $\sim 0.36$  keV. The addition of an emission line, suggested by the RGS spectra to be the C VI  $L_\alpha$  line at  $33.7 \text{ \AA}$ , matches better the CSPN spectrum with best-fit parameters  $T_X \approx 9.4 \times 10^5 \text{ K}$  and  $L_X \approx 1.2 \times 10^{32} \text{ erg s}^{-1}$ .

### 3 Results

The exquisite spatial resolution of *Chandra* and unprecedented sensitivity of *XMM-Newton* have allowed us to resolve the X-ray emission from A 30 into a point-source at its central star and diffuse emission associated with the innermost hydrogen-poor knots and with the cloverleaf structure inside the nebular shell. The spatial distribution and spectral properties of the diffuse X-ray emission from A 30 are highly suggestive that it originates in the interactions of the present fast stellar wind and post-born-again wind with the hydrogen-poor ejecta. After the born-again event, the hydrogen-poor, carbon-rich post-born-again wind blew a cavity into the nebula that resulted in the cloverleaf structure. The interactions of this wind and the present fast stellar wind with clumps of low speed and carbon-rich dust from the born-again event result in processes of shock-heating and mass-loading of the stellar winds and ablation of the hydrogen-poor knots that produce X-ray-emitting plasma. Charge-exchange reactions between the ions of the stellar winds and neutral or ionized hydrogen-poor material in knots

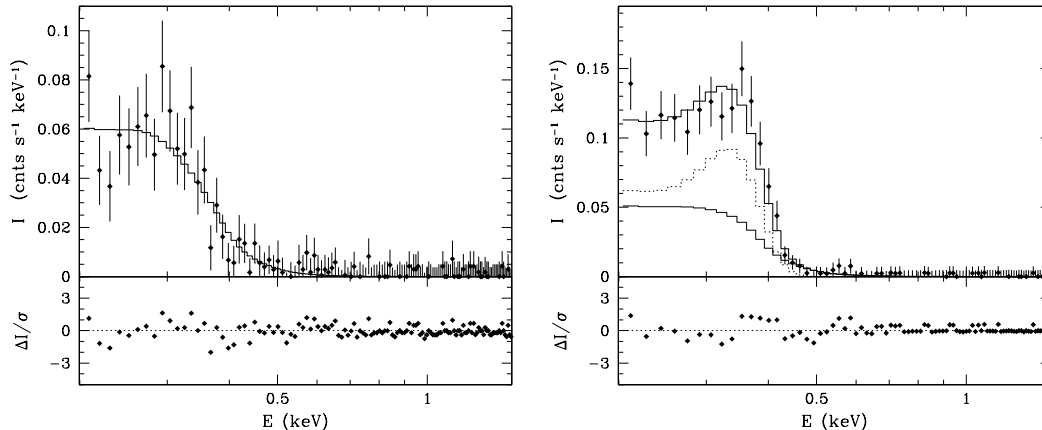


Figure 2: *XMM-Newton* background-subtracted spectra overplotted with best-fit models of the diffuse (*left*) and stellar (*right*) emissions. The latter shows the C VI emission line (dotted histogram) added to the thermal component with [15, Leuenhagen et al.’s (1993)] chemical abundances (thin histogram) that suggests higher carbon abundances than the diffuse emission.

and dust can also contribute to the production of this diffuse X-ray emission.

The origin of the X-ray emission from the central star of A 30 is puzzling. To help us assess the role of the current stellar wind in powering this X-ray emission, we have determined the stellar parameters and wind properties of the [WC] central star of A 30 using the Potsdam Wolf-Rayet (PoWR) model atmosphere code [9] to fit its optical and UV spectra. Our detailed atmosphere model shows that the large opacity of the stellar wind would severely obscure the X-ray emission from shocks in this wind to undetectable levels, as is also the case for the stellar wind of WC stars [16]. A photospheric origin can be ruled out, too, as the photospheric emission predicted by our non-LTE model is softer than the X-ray emission observed in A 30. The development of a new, compact hot bubble confining the fast stellar wind cannot be completely excluded in term of energetics, but its small size and consequent short age, a few  $\times 10$  yr, implied from the *Chandra* observations makes it implausible.

For further details, see a complete description of this research in [8].

## Acknowledgments

This work has been partially funded by grants AYA 2008–01934 and AYA2011–29754–C03–02 of the Spanish MICINN (Ministerio de Ciencia e Innovación) and MEC (Ministerio de Economía y Competitividad).

## References

- [1] Balick, B. 1987, *AJ*, 94, 671
- [2] Berghoefer, T. W., Schmitt, J. H. M. M., Danner, R., & Cassinelli, J. P. 1997, *A&A*, 322, 167

- [3] Borkowski, K. J., Harrington, J. P., & Tsvetanov, Z. I. 1995, *ApJ*, 449, L143
- [4] Chu, Y.-H. & Ho, C.-H. 1995, *ApJ*, 448, L127
- [5] Chu, Y.-H., Chang, T. H., & Conway, G. M. 1997, *ApJ*, 482, 891
- [6] Feldmeier, A., Puls, J., & Pauldrach, A. W. A. 1997, *A&A*, 322, 878
- [7] Guerrero, M. A. & Machado, A. 1996, *ApJ*, 472, 711
- [8] Guerrero, M. A., Ruiz, N., Hamann, W.-R., et al. 2012, *ApJ*, 755, 129
- [9] Hamann, W.-R. & Gräfener, G. 2004, *A&A*, 427, 697
- [10] Hazard, C., Terlevich, R., Ferland, G., Morton, D.C., & Sargent, W.L.W. 1980, *Nature*, 285, 463
- [11] Iben, I., Jr., Kaler, J. B., Truran, J. W., & Renzini, A. 1983, *ApJ*, 264, 605
- [12] Jacoby, G.H. 1979, *PASP*, 91, 754
- [13] Jacoby, G. H. & Ford, H. C. 1983, *ApJ*, 266, 298
- [14] Kwok, S., Purton, C. R., & Fitzgerald, P. M. 1978, *ApJ*, 219, L125
- [15] Leuenhagen, U., Koesterke, L., & Hamann, W.-R. 1993, *AcA*, 43, 329
- [16] Oskinova, L. M., Hamann, W.-R., Feldmeier, A., Ignace, R., & Chu, Y.-H. 2009, *ApJ*, 693, L44
- [17] Oskinova, L. M., Ignace, R., Hamann, W.-R., Pollock, A. M. T., & Brown, J. C. 2003, *A&A*, 402, 755
- [18] Schönberner, D., Jacob, R., Sandin, C., & Steffen, M. 2010, *A&A*, 523, A86